5.4 Measurement methods

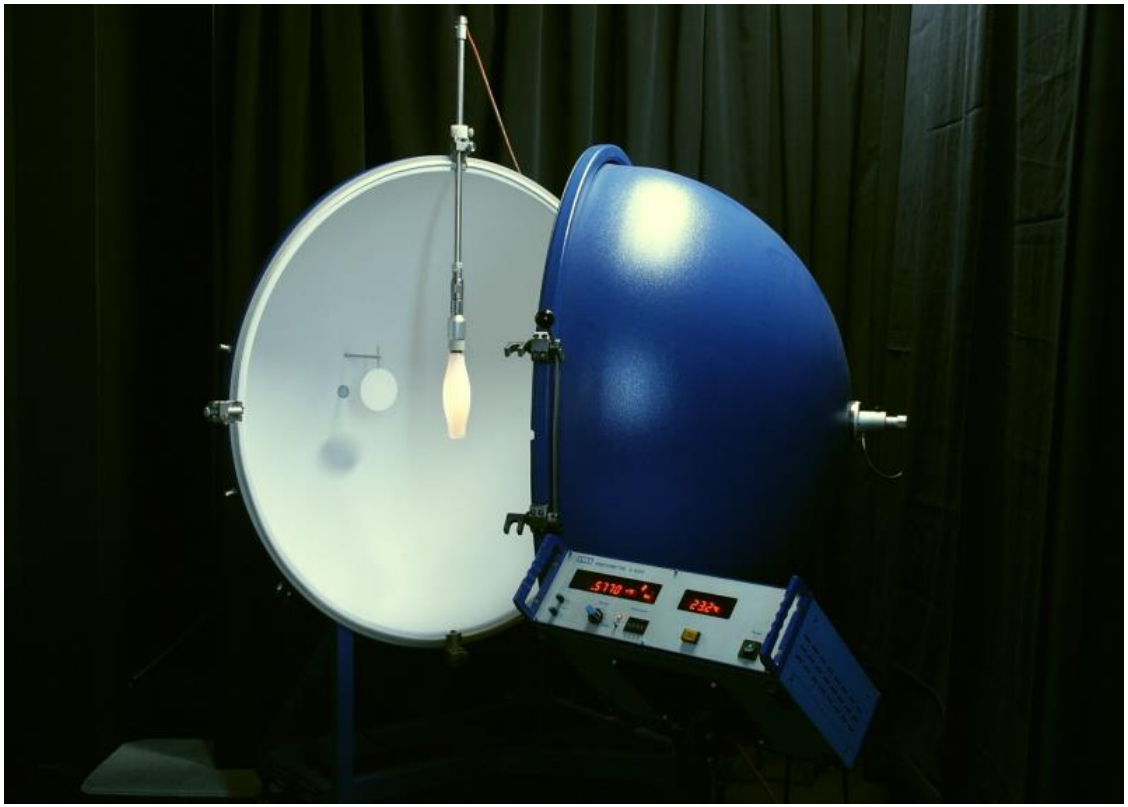

Two approaches are used to measure the optical properties of biological tissues:

Direct methods:

direct measurement of μ_a, μ_s, $p(\theta)$. These methods do NOT require the use of a model !

Indirect methods:

based on the use of models describing the propagation of light. An inverse problem has to be solved to get the fundamental parameters.

Direct methods

Performed on "thin" samples ($d < 1/\mu_t$) to prevent multiple scattering.

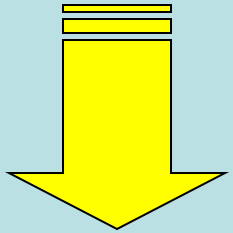

$(\mu_t = \mu_a + \mu_s)$

Direct methods are not suited for *in vivo* measurements.

! Degradation of the sample + heterogeneities !

Direct methods:

Measurement of $\mu_t = \mu_a + \mu_s$

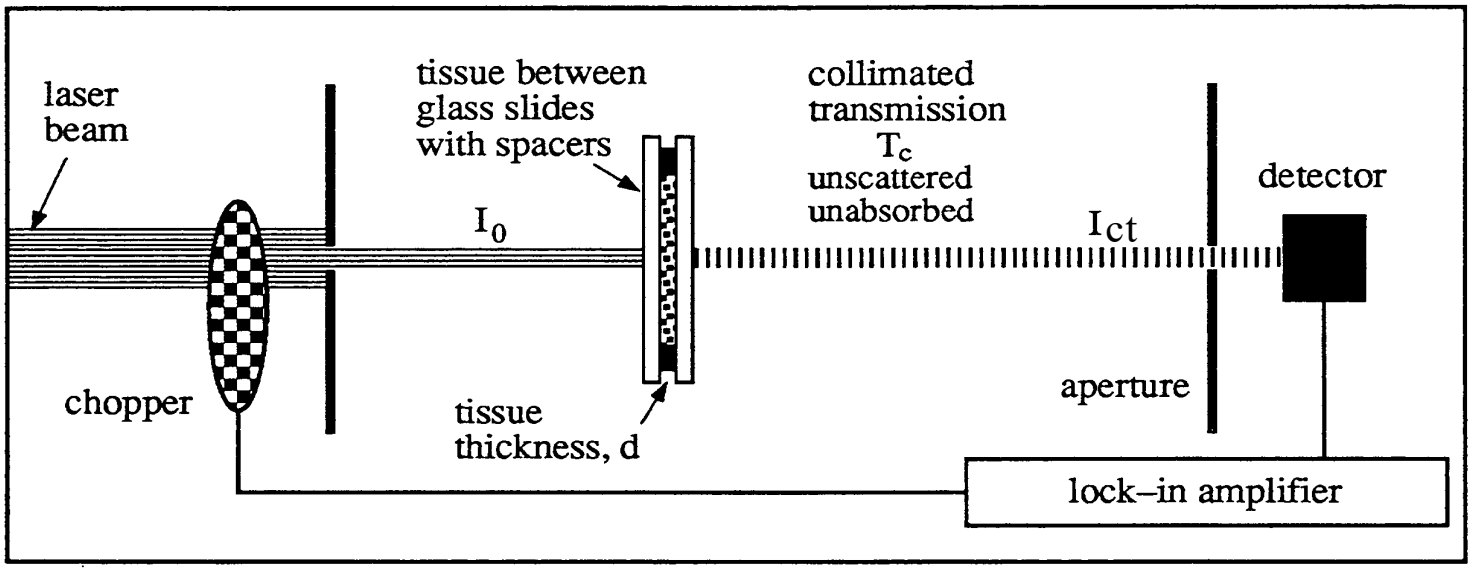

$$\mu_t = -\frac{1}{d} \ln\left(\frac{I_{ct}}{I_0}\right)$$

Solid angle of the detector: about 10^{-5} sr !

Direct methods:
Measurement of μ_t

"T 380" Tumor
at 630 nm

Sample thickness: d [mm]

Slope = μ_t

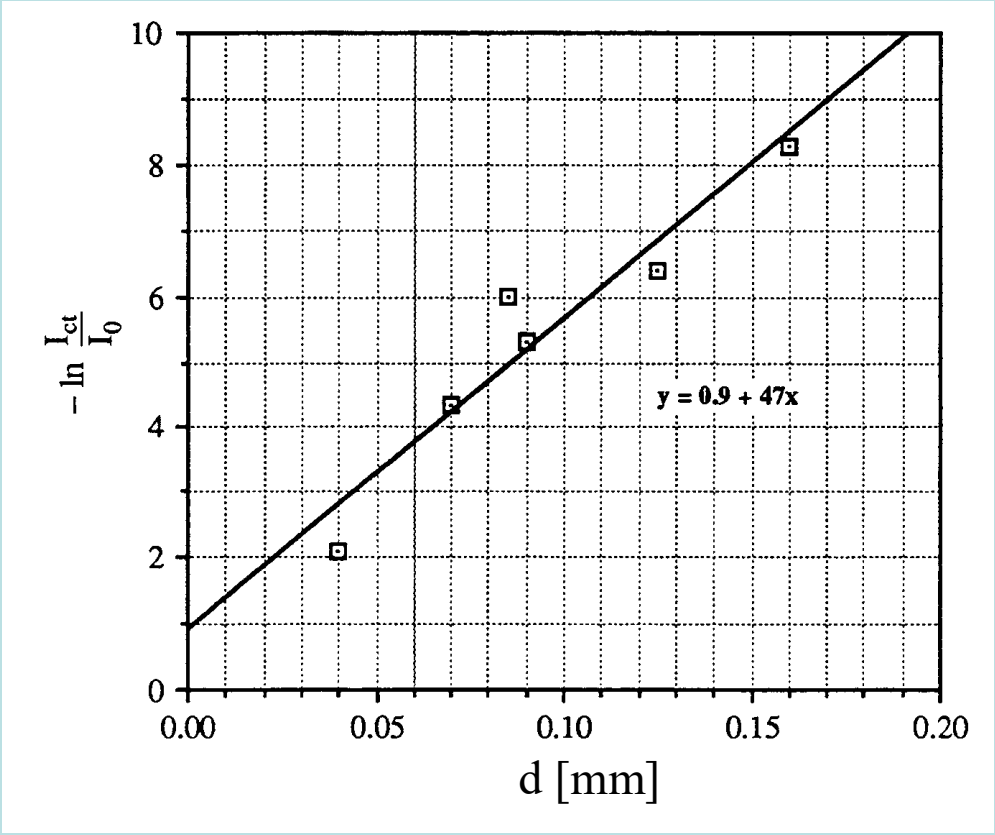

Direct methods:
Measurement of p(θ)

Angular scattering experiment: Goniometer

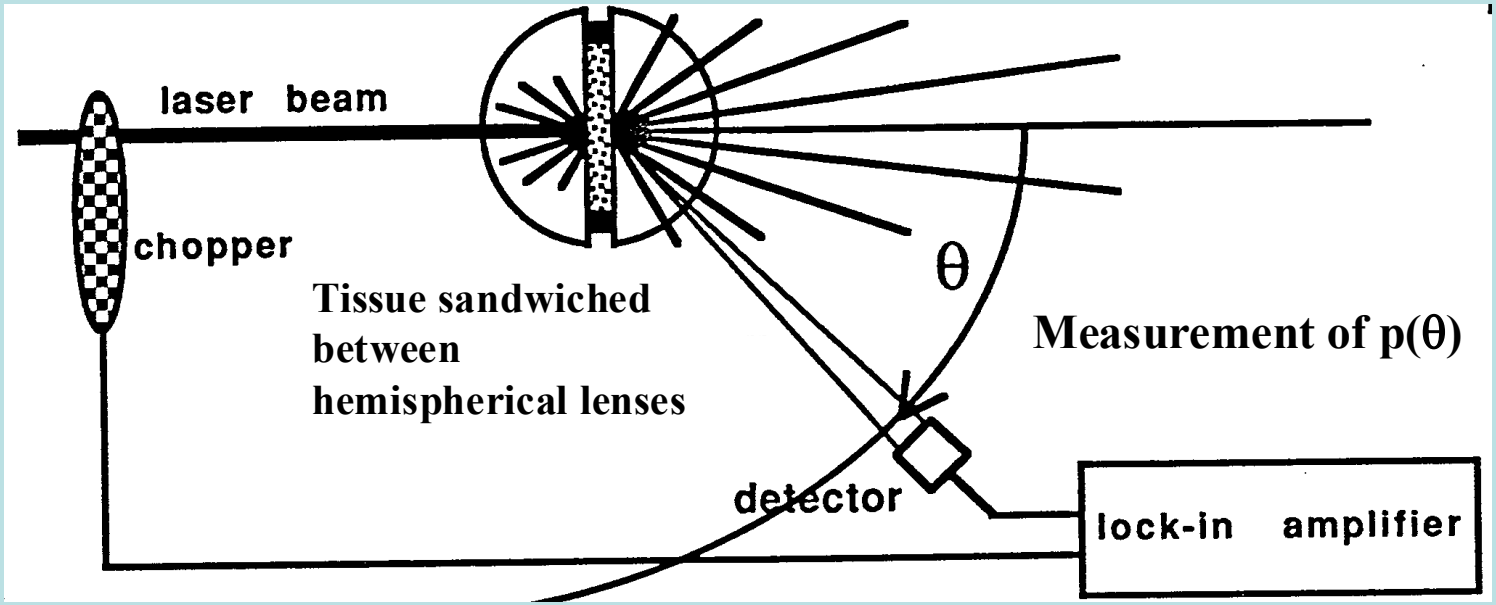

Direct methods: Measurement of μ_s

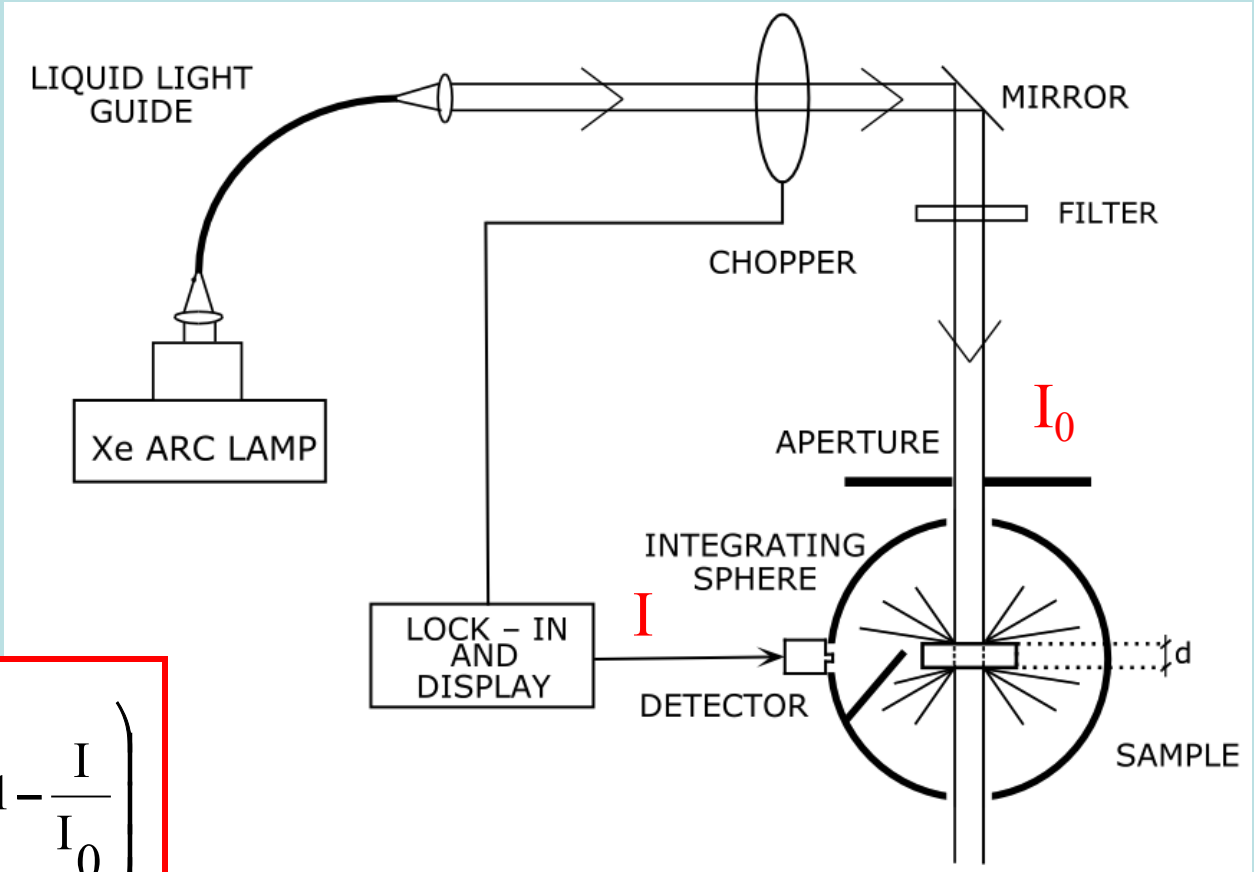

If $\mu_a \ll \mu'_s$

$$\mu_s = -\frac{1}{d}\ln\left(1-\frac{I}{I_0}\right)$$

!! Specular reflections must be avoided !!

Direct methods: Measurement of μ_a

If μ_a is larger than μ'_s

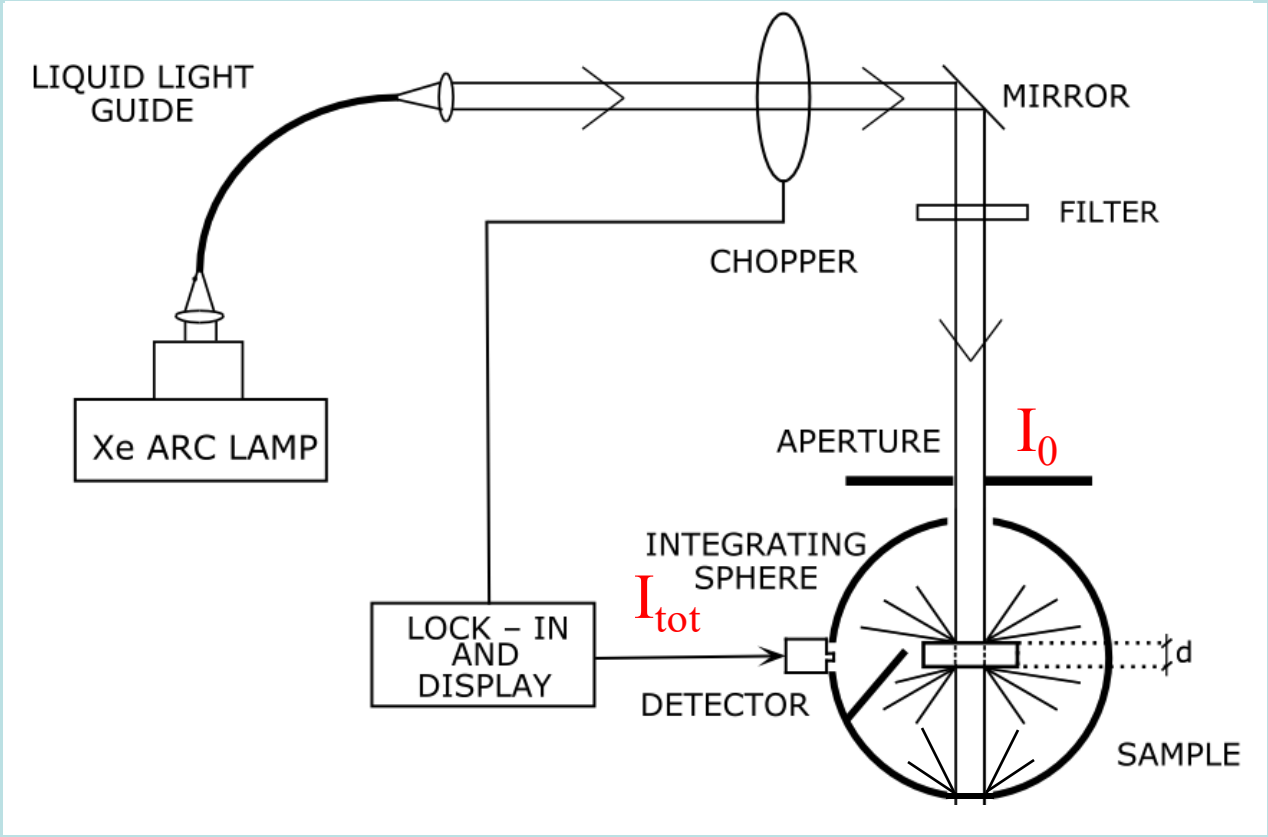

$$\mu_a = -\frac{1}{d} \ln\left(\frac{I_{tot}}{I_0}\right)$$

!! Specular reflections must be avoided !!

Indirect methods

Can be performed on thick samples.

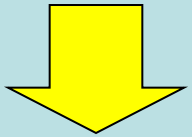

- **Suited for *in vivo* measurements.**
- **Less sensitive to tissue heterogeneities than the direct methods.**

But: Experimental conditions must be compatible with the hypothesis of the model used to derive the parameters ! (to solve the inverse problem)

The indirect methods

... can be classified in three categories:

1. **The "internal" approaches**
   where the detector is inserted in the tissue
2. **The "external" approaches**
   where the detector is positioned outside the tissue (non invasive)
3. **The approaches**
   based on the use of added absorbers

General comments

- These indirect approaches can be based on steady-state or time-resolved methods.
- This is most frequently μ_{eff} that is extracted from steady state diffusion in bulk tissues.
- The extraction of μ_{eff} is frequently based on the use of the diffusion approximation equation.
- The g-value can never be evaluated with the diffusion theory.

Indirect methods:

1) Internal approach: direct measurements of the fluence rate

A technique frequently used to evaluate μ_{eff} $\mu_{eff} = \sqrt{3\mu_a(\mu_a + \mu_s')}$ from steady state measurements is to directly measure the fluence rate.

To do that one

- needs to be inside the tissue
  ==> invasive measurements.
- needs to measure light coming from all directions
  ==> isotropic detector.

$$\phi(r,t) = \int_{4\pi} L(r,s,t)\, d\theta$$

Radiance L (**r**, **s**, t)
= amount of light that passes through a particular area, and falls within a given solid angle

Isotropic light detector

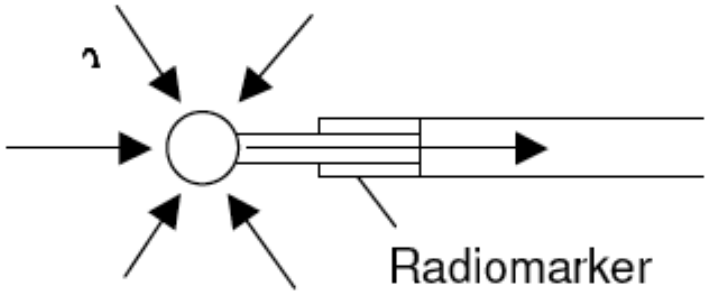

The isotropy results from the scattering of light in the spherical tip !

TECHNICAL DATA

MECHANICAL DIMENSIONS	IP85	IP159
OD DISTAL TIP	0.85 mm (1/30")	1.59 mm (1/16")
OVERALL LENGTH	3 m	3 m
OPTICAL CHARACTERISTICS		
ISOTROPY (standard deviation from 40° to 320°, in air)	± 10%	± 10%
WAVELENGTH RANGE	480 – 800 nm	480 – 800 nm
OPTICAL FIBER		
FIBER MATERIAL	SILICA, low OH^-	SILICA, low OH^-
CORE DIAMETER	400 µm	400 µm
NUMERICAL APERTURE	0.37	0.37
MINIMUM BENDING RADIUS	47 mm	47 mm
FIBER CONNECTOR	SMA 905	SMA 905

Indirect internal methods: Measurement of the fluence rate: Detectors

Characteristics of isotropic detector

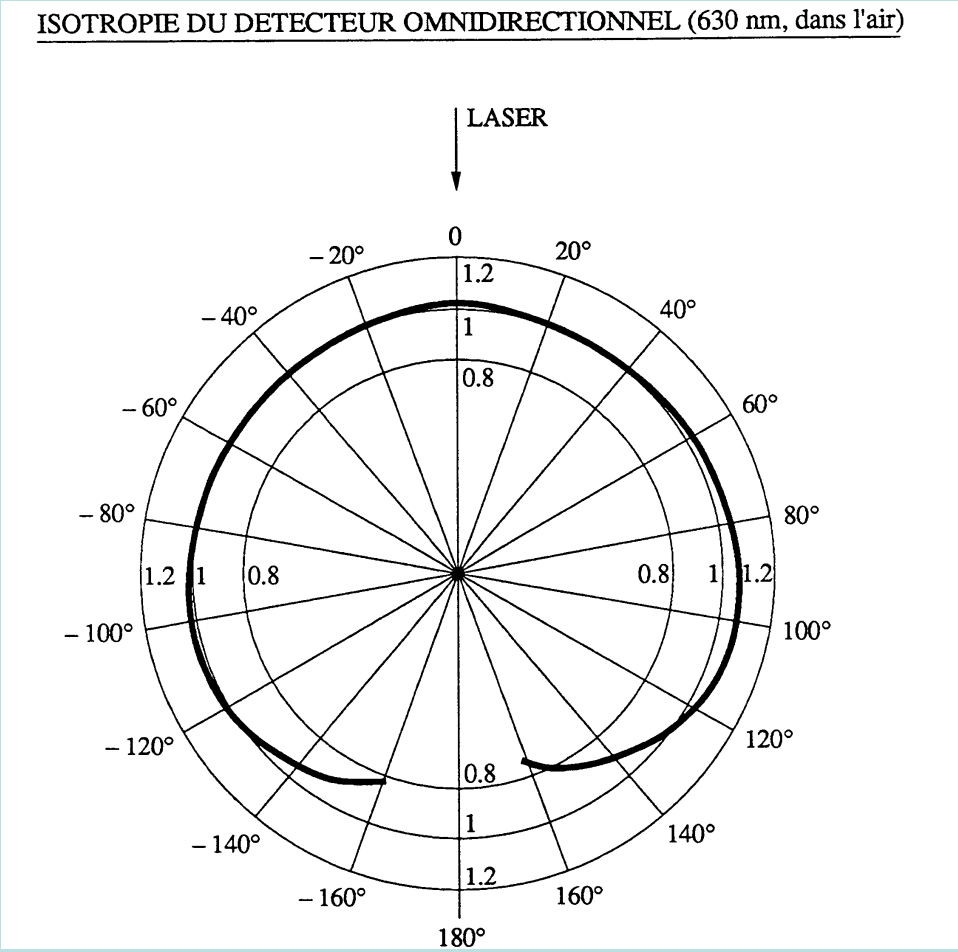

Indirect internal methods:
Typical example: Measurement of μ_{eff}

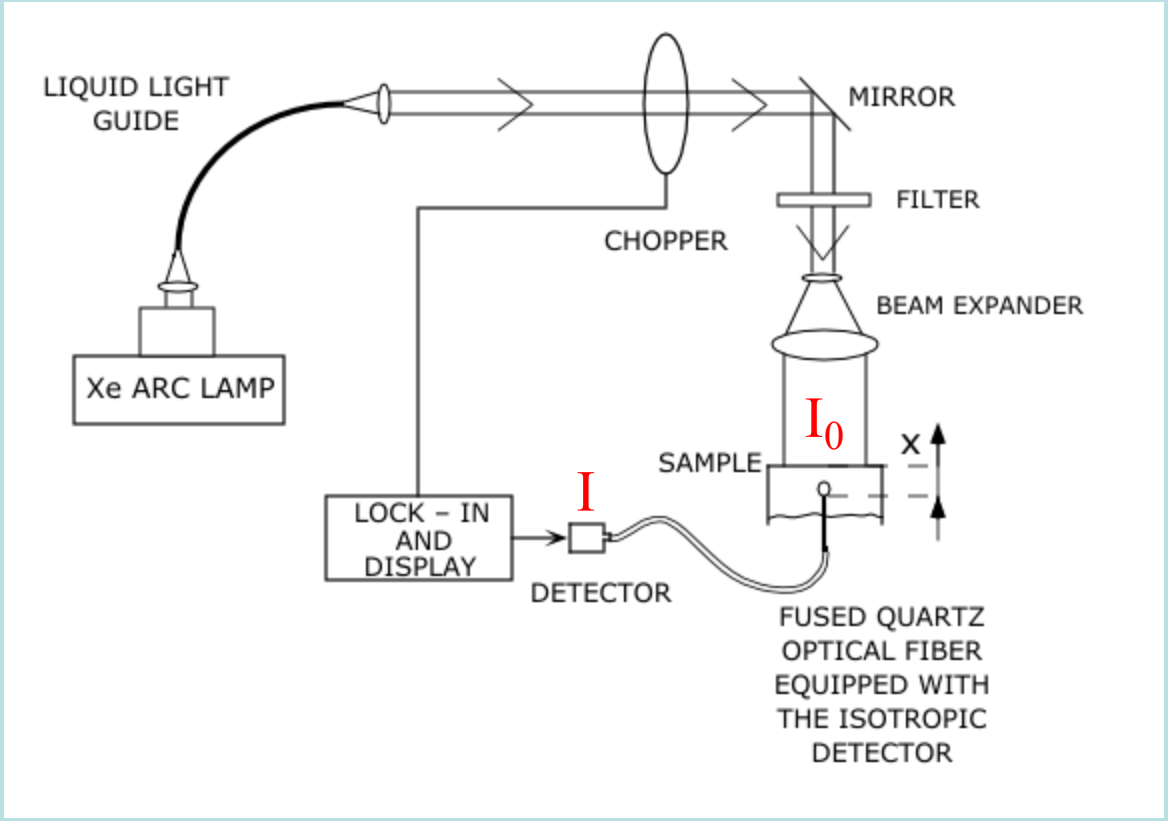

Collimated "Broad" illumination perpendicular to the air-tissue interface

Semi-infinite volume of tissue

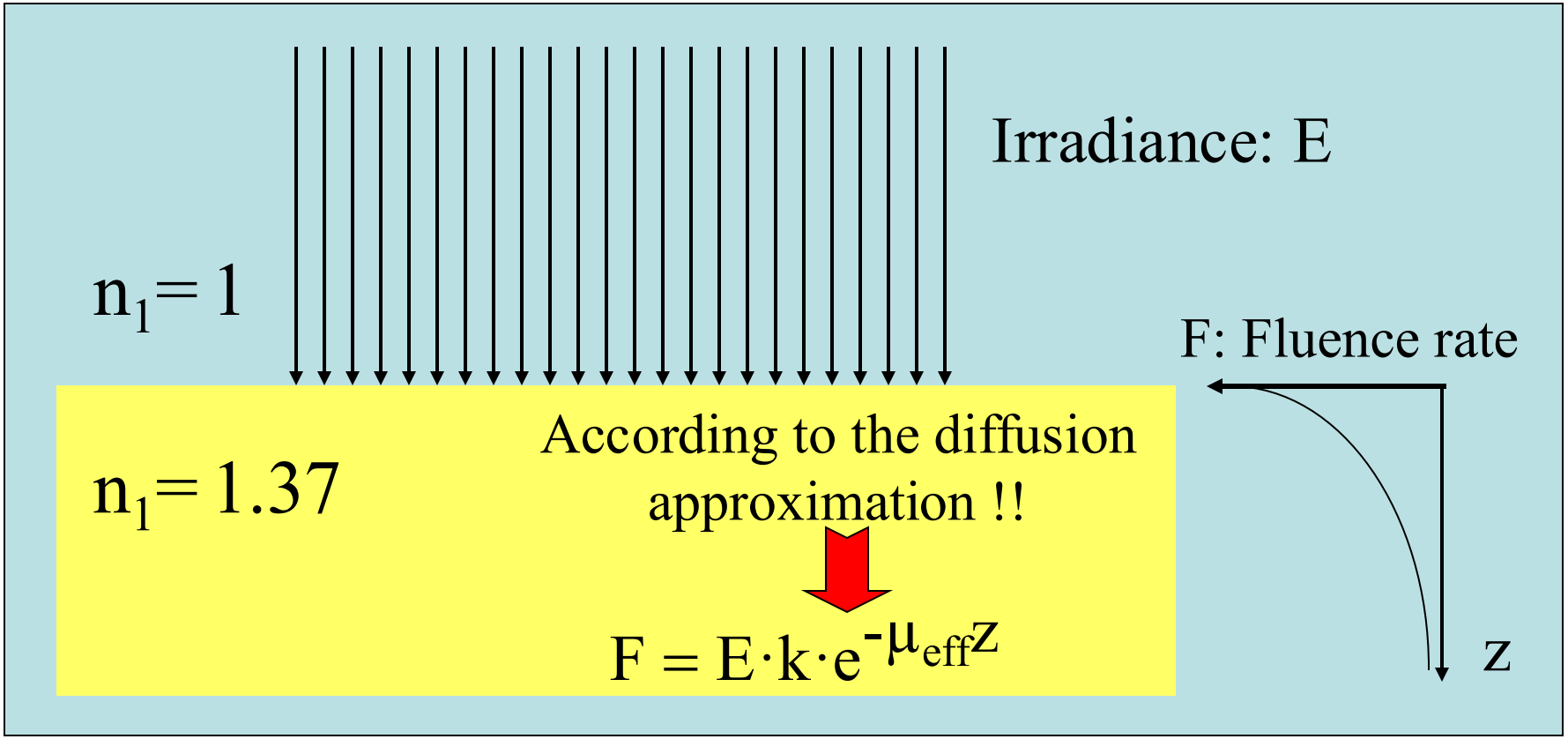

Indirect internal methods:
Example - Measurement of μ_{eff}

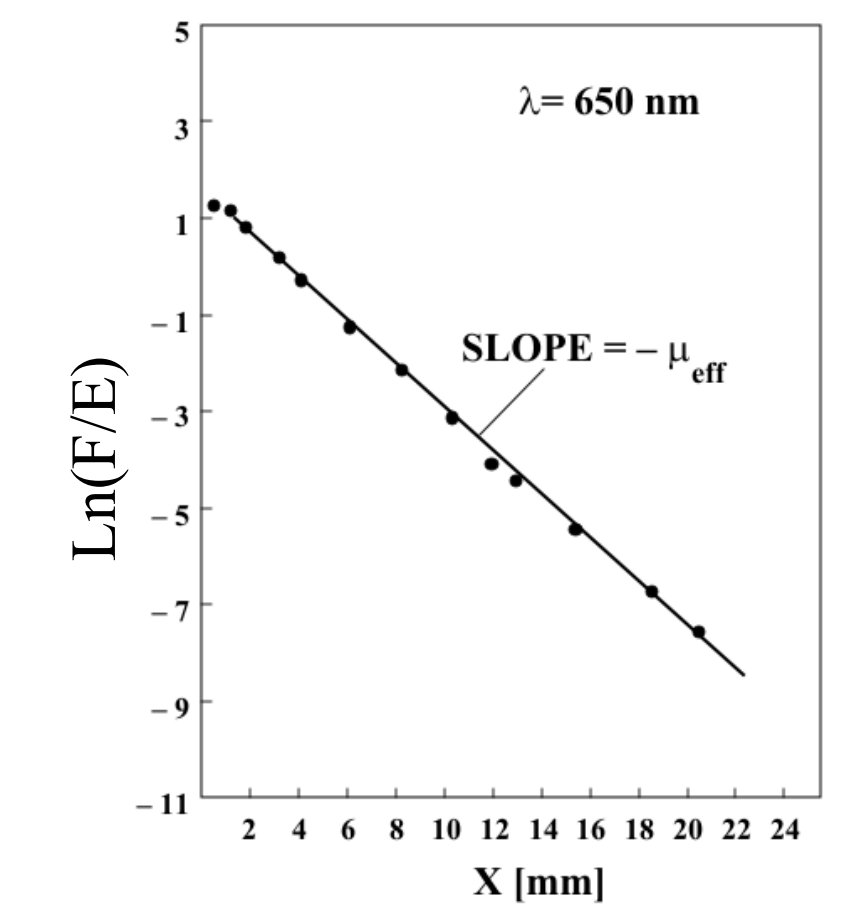

Beef muscle (ex vivo)

$\mu_{eff} = 0.45\ mm^{-1}$

Indirect internal methods:
Measurement of the fluence rate

Isotropic light detector
based on the fluorescence of the distal tip

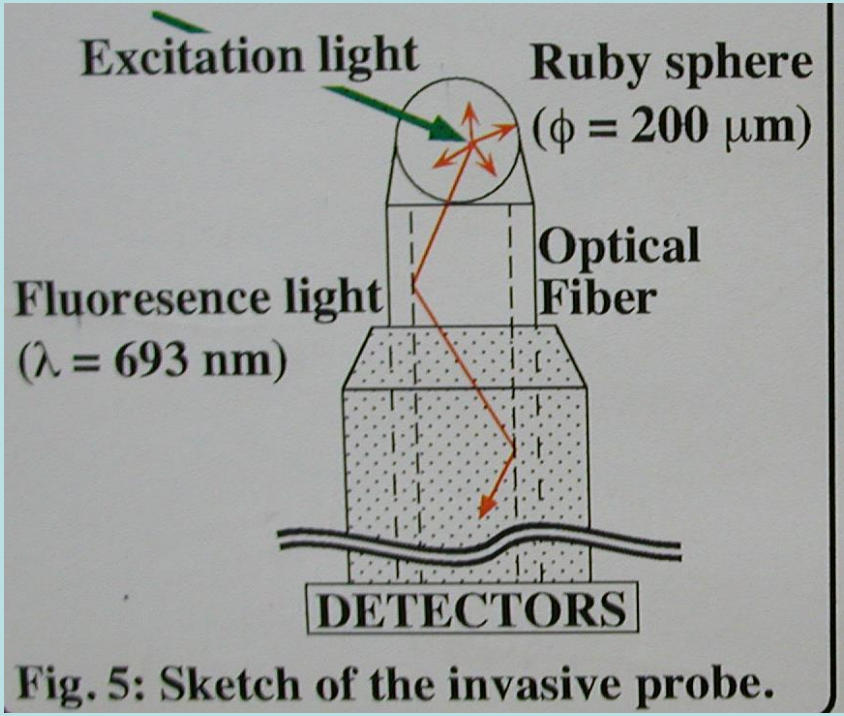

Fig. 5: Sketch of the invasive probe.

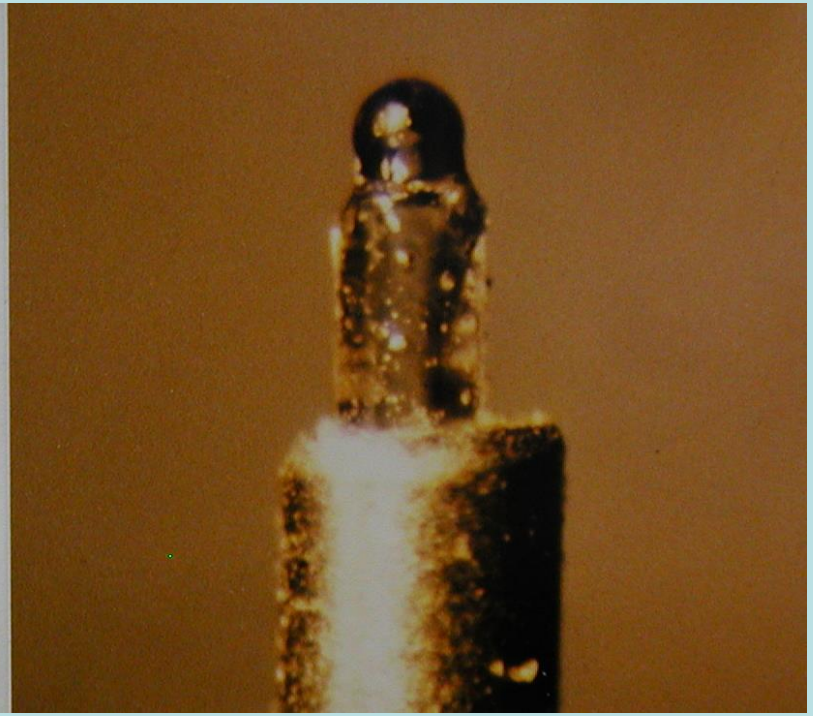

Indirect internal methods – Clinical example: Measurement of fluence rate in the cheek of a volunteer

... using an isotropic light detector based on the ruby's fluorescence

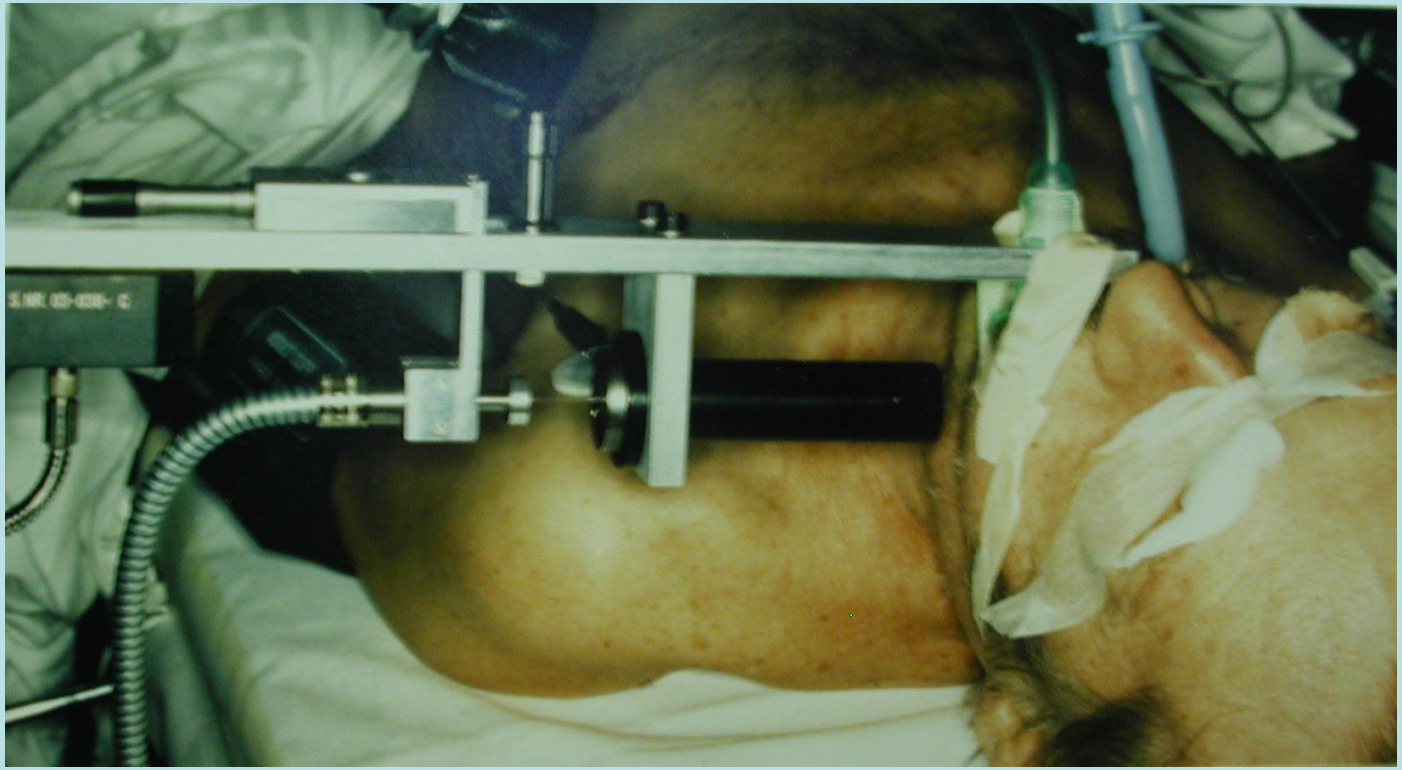

Indirect internal methods – Clinical example: Measurement of the fluence rate in the cheek of a volunteer

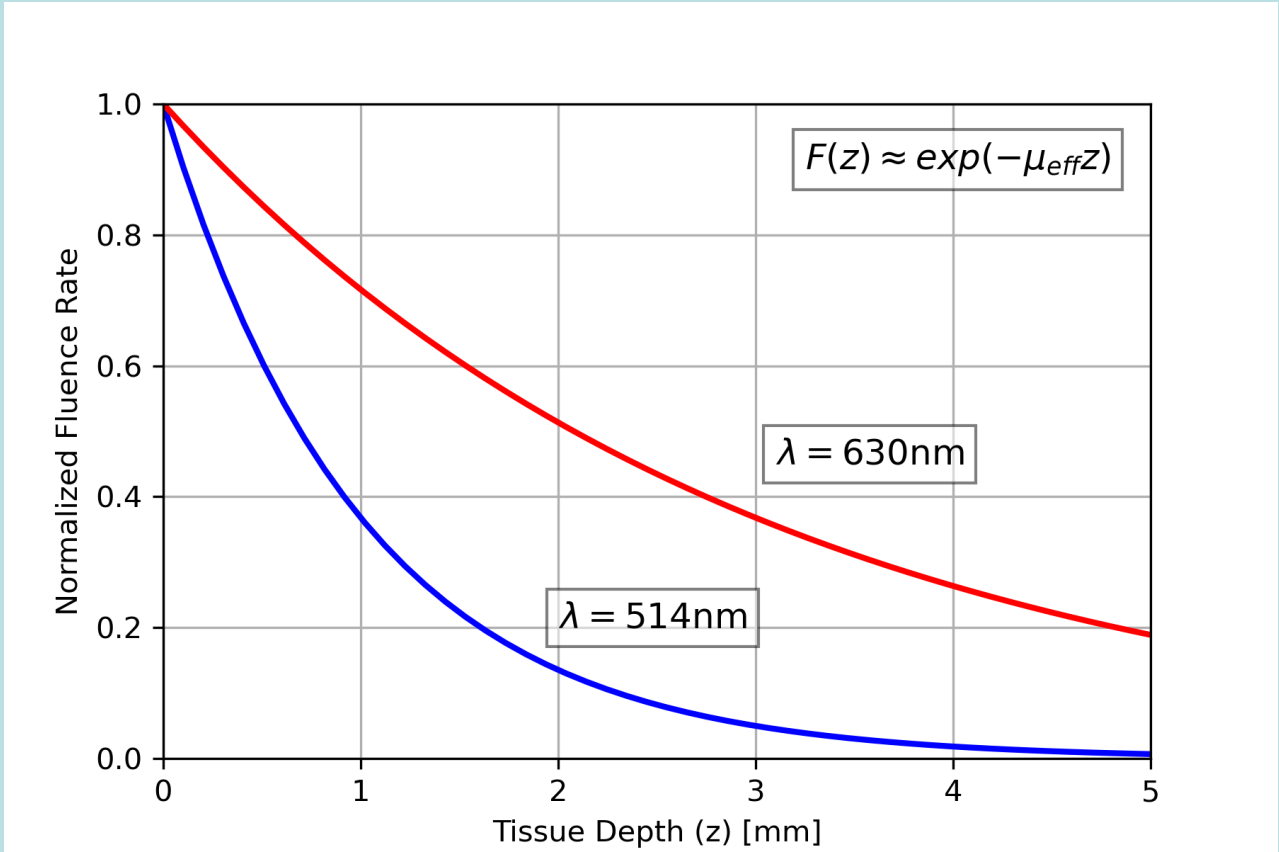

Indirect methods:
2) External approach

- Spatially resolved CW measurements
- Integrating sphere measurements (Kubelka-Munk)
- Time-resolved measurements

Indirect methods:
Spatially resolved CW Reflectometry

- This method is an alternative, non-invasive way to measure the **r-dependence of the fluence rate**.
- By measuring at a boundary, one needs to take the boundary conditions into account.

Indirect methods:
Spatially resolved CW reflectometry

Determination of the parameters using:

- Diffusion equation - curve fitting
- Monte Carlo method - curve fitting
- Calibration against known standards

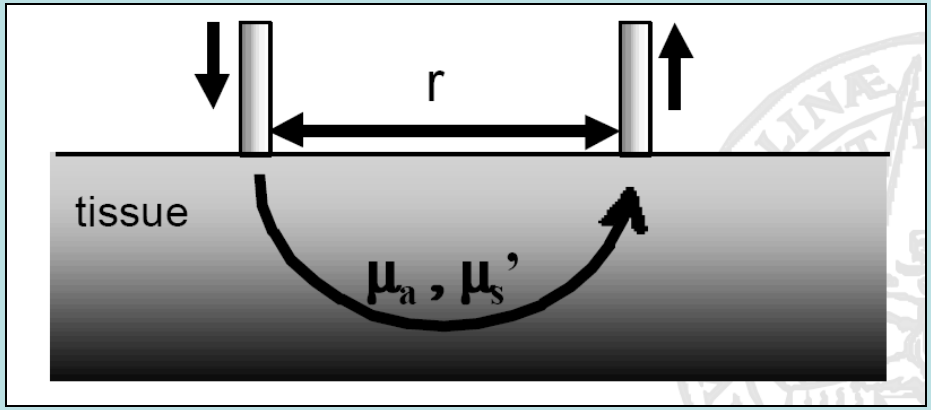

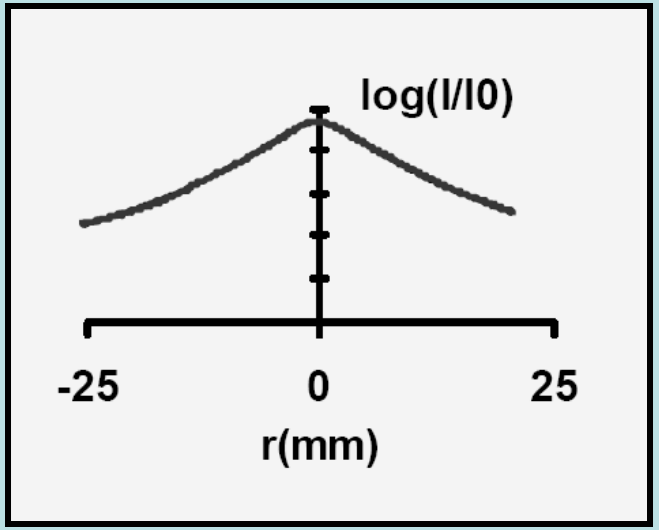

Spatially resolved CW reflectometry
Diffuse reflectance equation

$$R(r) \propto D_1 r^{-1/2} \exp(-D_2 r)$$

- D_1 and D_2 parameters are determined from the light propagation model.
- The calculated values of D_1 and D_2 are then compared with those obtained by fitting the experimental measurement with the model.

$D_x = D_x(\mu_a, \mu_s', n, \text{geometry})$; $x = 1, 2$

R. Bays, Thesis EPFL Nr. 1086

Spatially resolved CW reflectometry

Where to probe the tissue ?

"Hinge" and "pivot" points

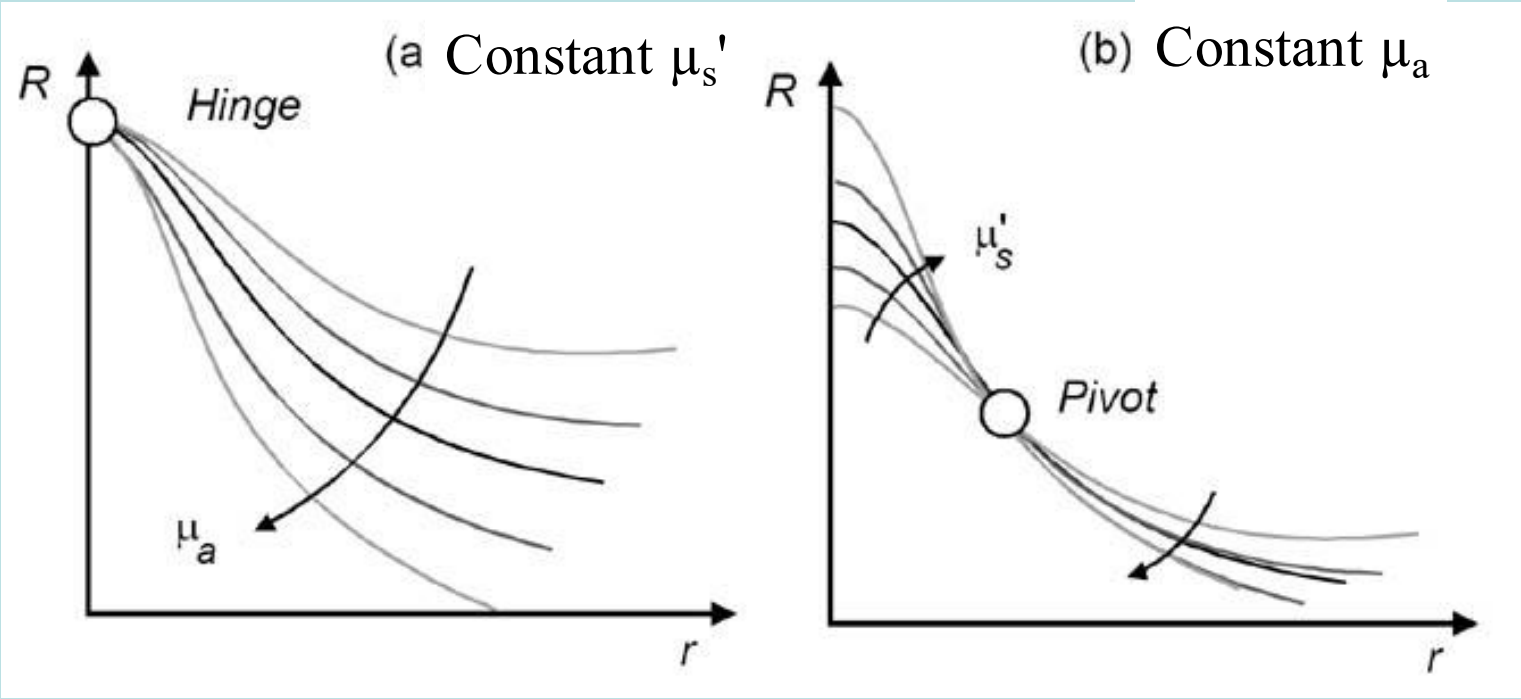

Spatially resolved CW reflectometry

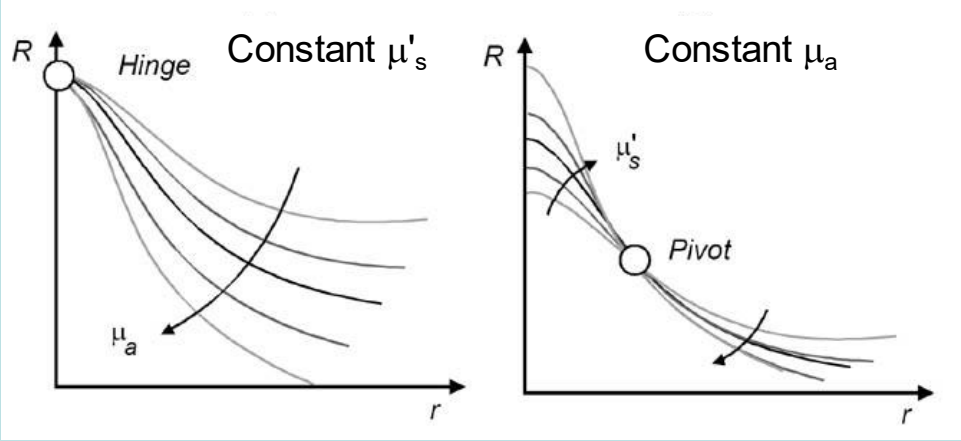

Optimal distances to measure μ'_s and μ_a :
one at the "hinge" and one beyond the "pivot" point

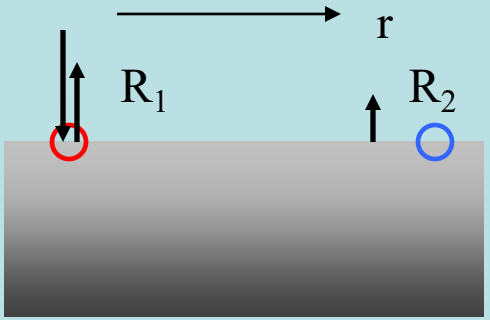

Spatially resolved CW reflectometry

Non-invasive probe for the esophagus

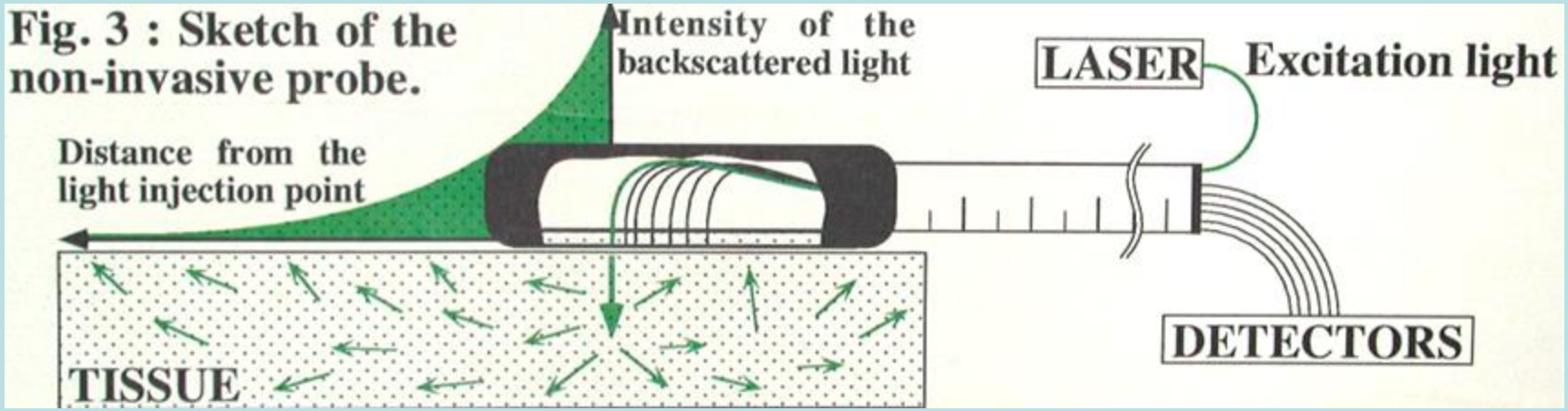

Spatially resolved CW reflectometry

Non-invasive probe for the esophagus

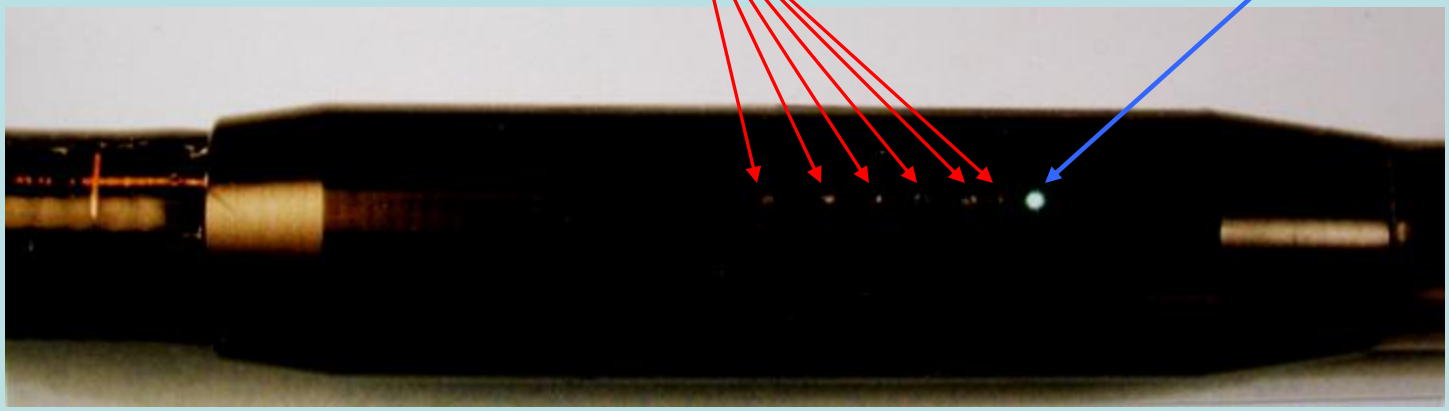

Diameter: 18 mm

Spatially resolved CW reflectometry Clinical example

Measurement in the oesophagus

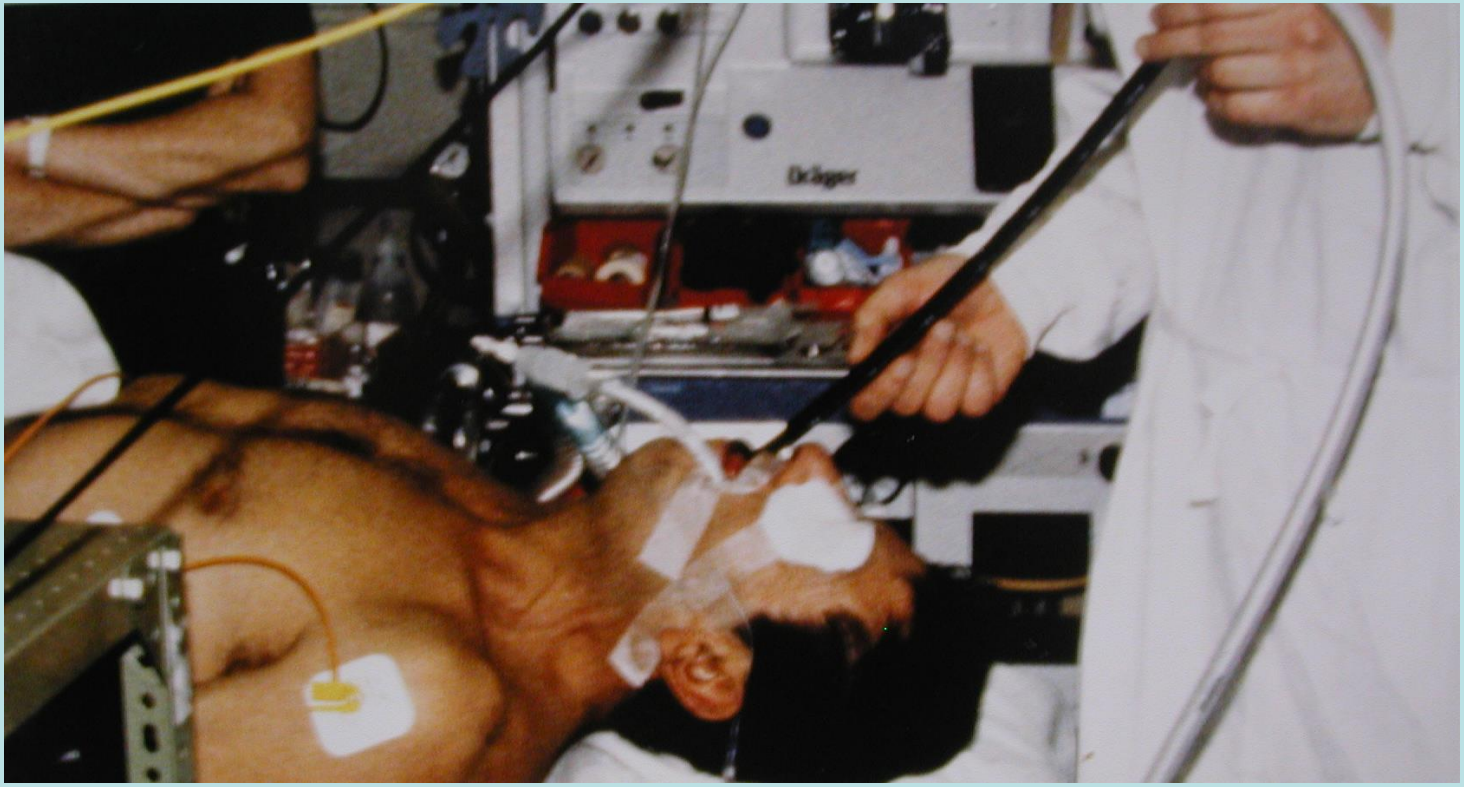

Set-up for spatially resolved reflectometry: Imaging detection

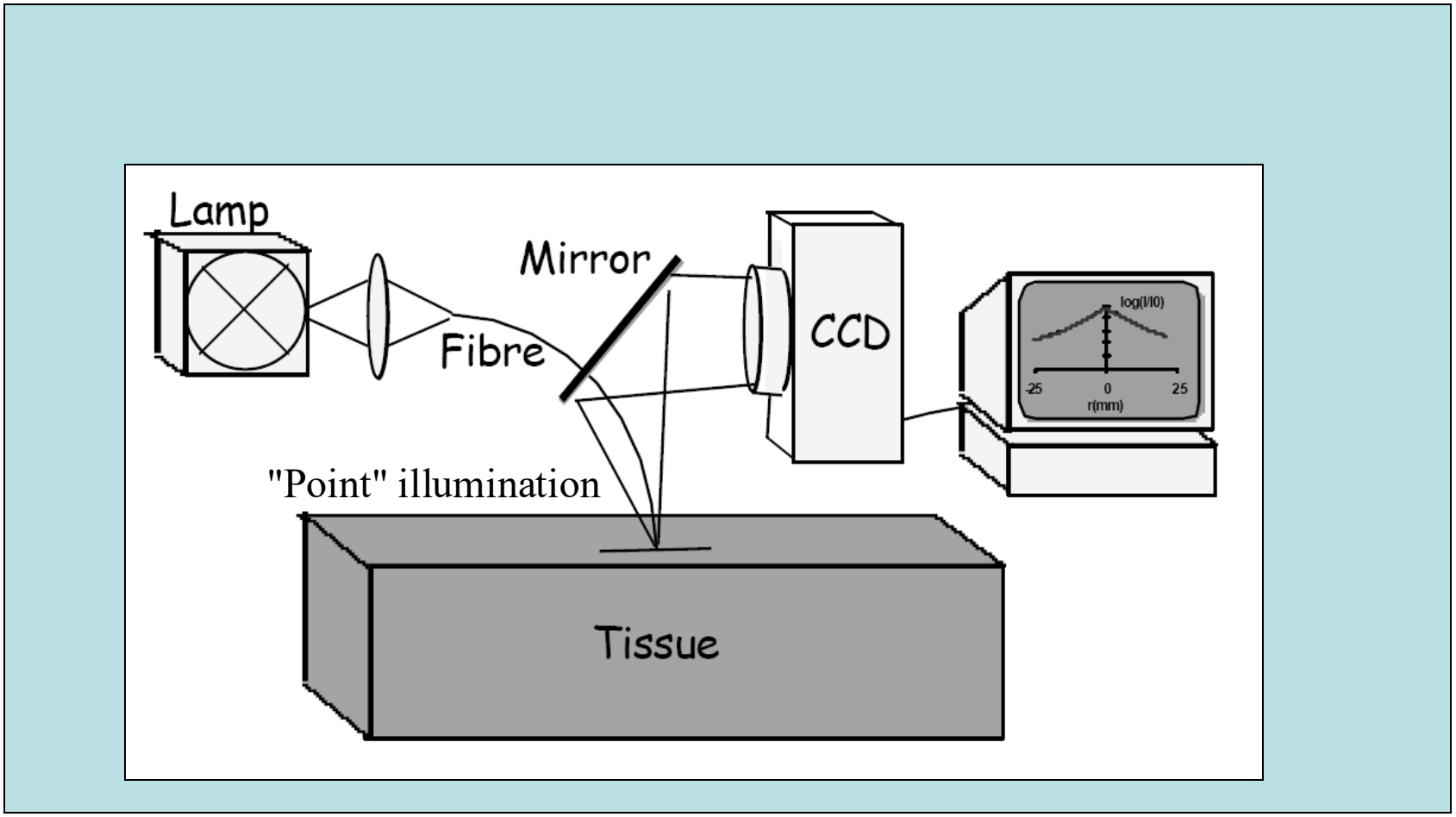

Spatially resolved reflectometry

Diffuse Reflectance from Skin

Diffuse reflectance of normal skin irradiated with a pencil beam of light, measured as line across the irradiated spot.

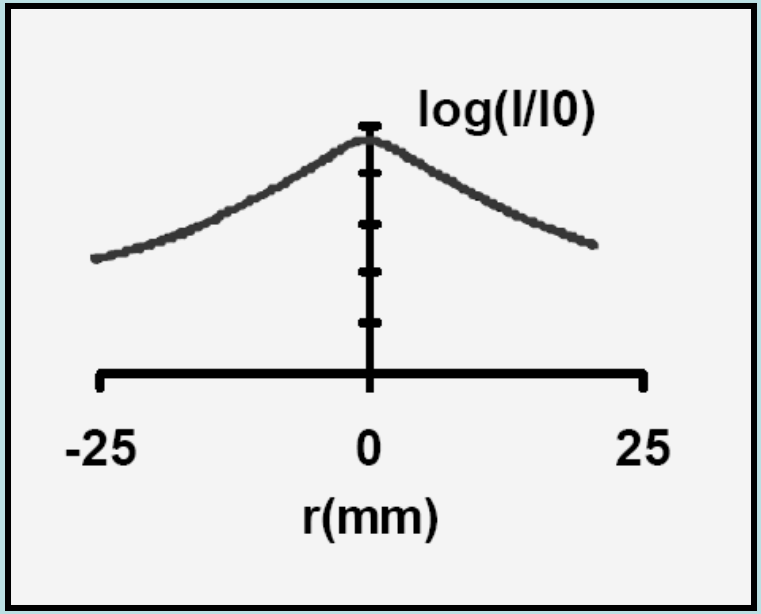

Measurements at a given wavelength can be performed with a filtered camera and a white light illumination !

Integrating sphere measurements

Kubelka-Munk (2-flux theory; diffuse illumination)

Setup to measure the diffuse reflectance R_{dt} and the diffuse transmittance T_{dt} of a "thick" sample

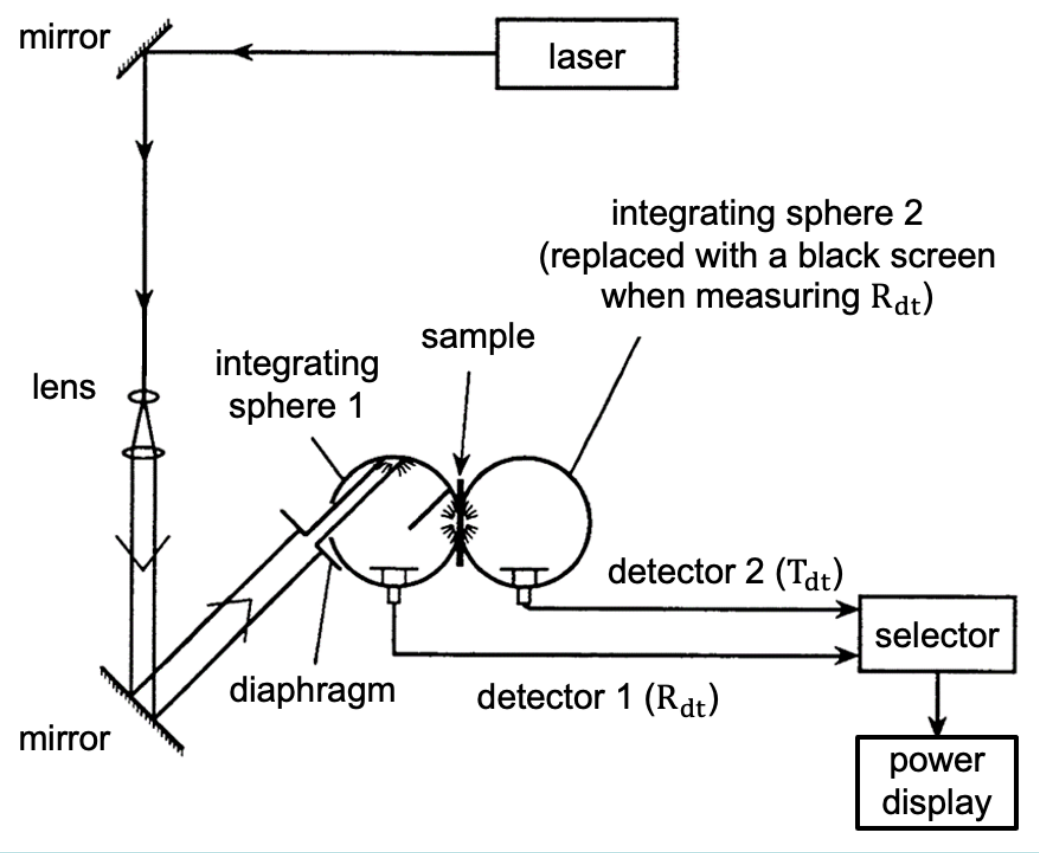

$$R_{dt} = \frac{I_1(\text{sample})}{I_1(100\%)}$$

$$T_{dt} = \frac{I_2(\text{sample})}{I_2(100\%)}$$

Where:

$I_1(100\%)$ = signal measured with the detector 1 when the tissue sample is replaced by a white reflecting (100%) coating.

$I_2(100\%)$ = signal measured with the detector 2 when the tissue sample is removed.

Integrating sphere measurements

Kubelka-Munk Theory (2-flux theory; diffuse illumination)

The Kubelka-Munk absorption and scattering coefficients may be directly expressed in terms of the measured reflection R and the transmission T.

$$S = \frac{1}{\sqrt{a^2 - 1}\cdot d}\cdot \ln\left(\frac{1 - R\left(a - \sqrt{a^2 - 1}\right)}{T}\right) \quad \text{and} \quad K = (a-1)\,S$$

$$\text{with} \quad a = \frac{K+S}{S} = \frac{1 + R^2 - T^2}{2R}$$

$$\mu_a = \eta\, K \qquad \mu_s' = \mu_s(1-g) = \chi\, S$$

M.J.C. van Gemert and W.M. Star, "Relations between the Kubleka-Munk and the transport equation models for anisotropic scattering", Lasers Life Sci, 1(4), (1987), pp.287-298

Integrating sphere measurements
Collimated illumination

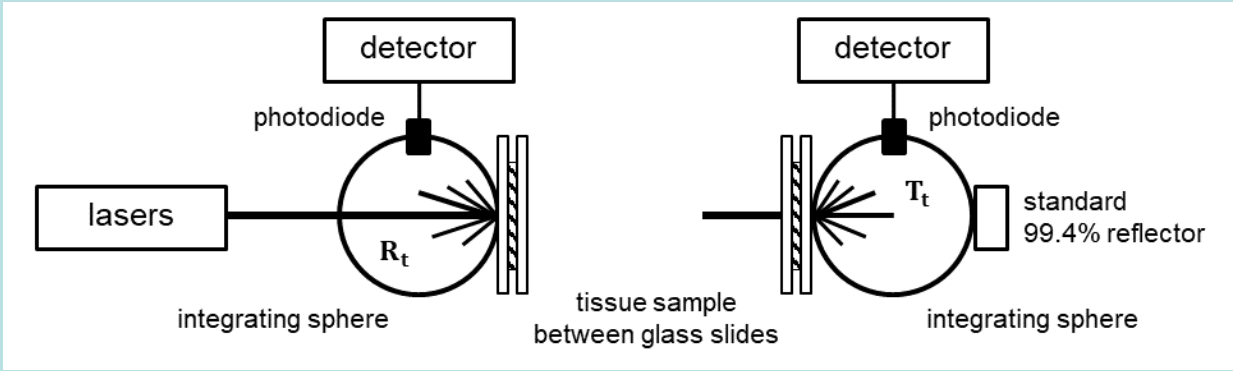

Monte-Carlo simulation

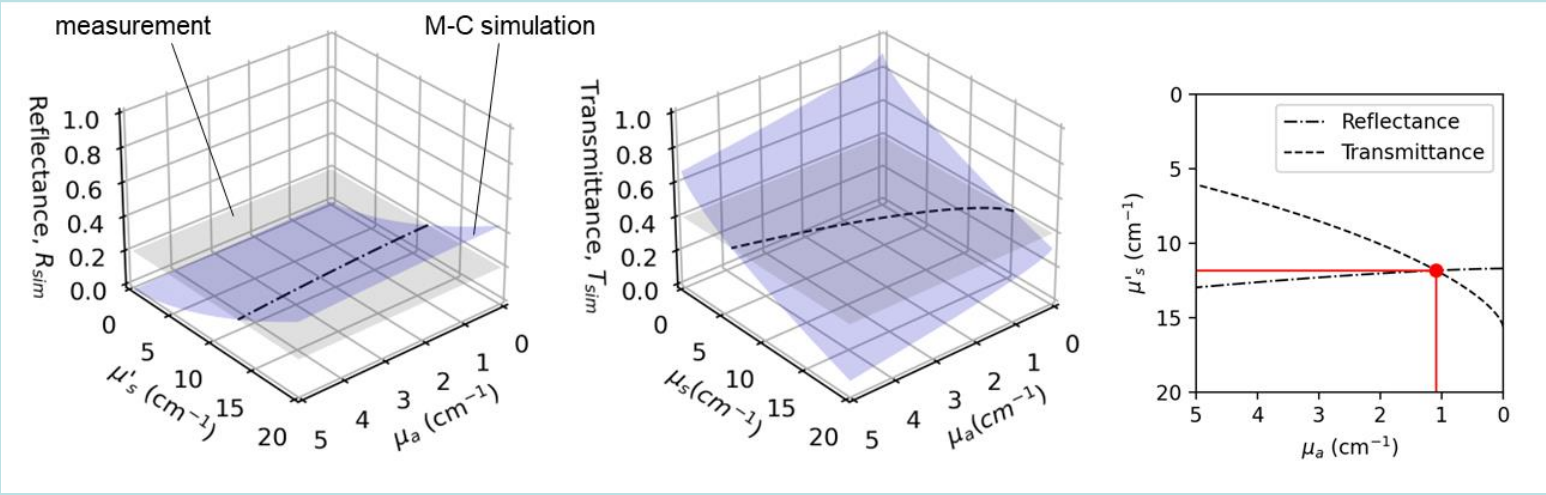

μ_a
μ'_s

External approach:
Time (and spatially) resolved reflectometry

Determination of the parameters using:

- Diffusion equation - curve fitting
- Monte Carlo method - curve fitting
- Calibration against known standards

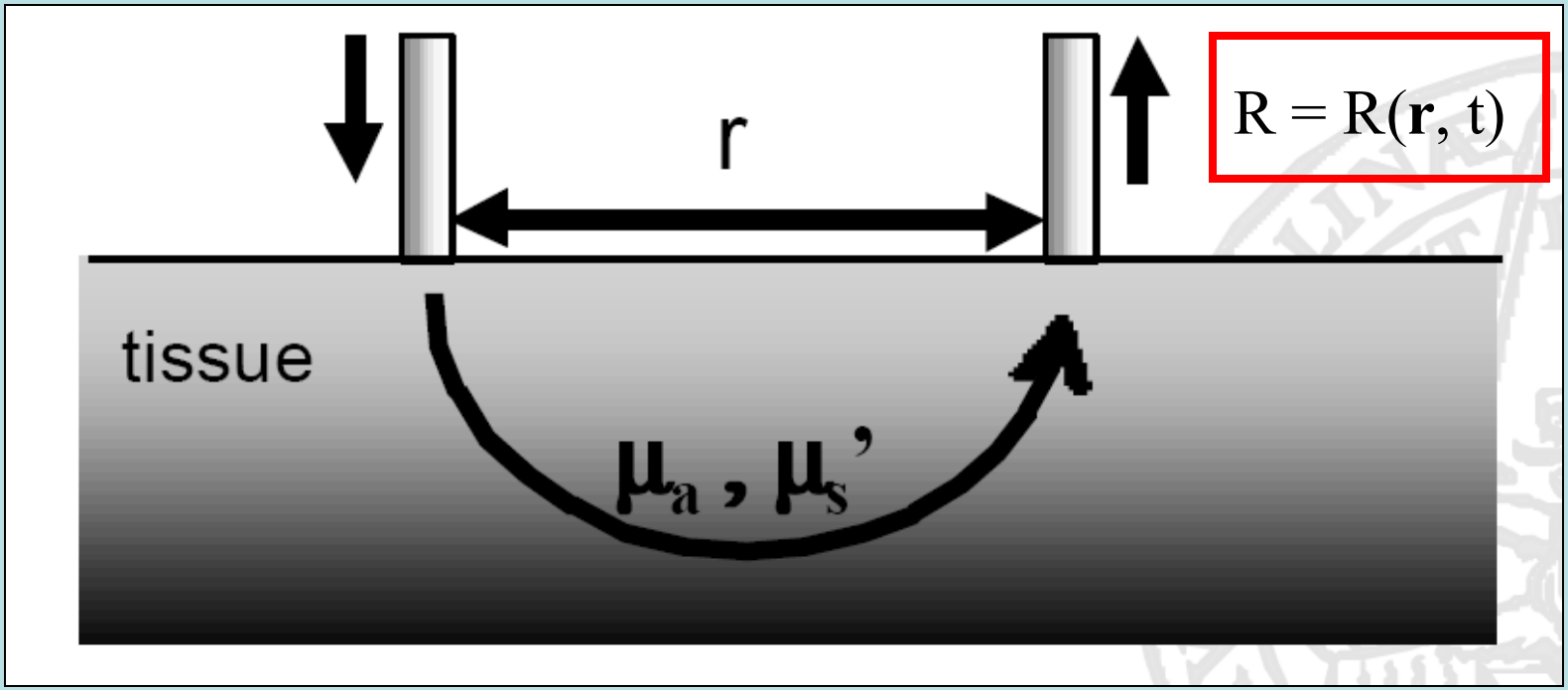

Time resolved reflectometry/transillumination: Motivation

Time- and spatially resolved reflectometry provides more information than the CW approach.

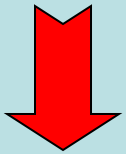

More robust and precise determination of μ_a despite light scattering.

References

Kienle and Patterson *J Opt Soc Am A 14 246-54 (1997)*
Kienle et al. *Appl. Optics 37 779-91(1998)*
Patterson et al. *Appl Optics 28 2331-36 (1998)*
Hyde et al. *Phys Med Biol 46 369-83 (2001)*

Time resolved reflectometry

- Reflectance measurements when made at the mismatched air/tissue surface boundary
- Local time-resolved reflectance R(r,t) for a semi-infinite medium
  (deduced from the diffusion approximation)

$$R(r,t) = (4\pi Dc)^{-3/2}(\mu_s')^{-1}t^{-5/2}\exp\left[-\frac{r^2+(\mu_s')^{-2}}{4Dct}\right]\exp(-\mu_a ct)$$

$$D = \frac{1}{3(\mu_a+\mu_s')} \qquad \mu_s' = \mu_s(1-g)$$

Time resolved reflectometry

- Total time-resolved reflectance R(t) for a semi-infinite medium (deduced from the diffusion approximation)

$$R(t) = \int_0^{\infty} R(r,t)\,2\pi r\,dr = (4\pi Dc)^{-1/2}(\mu_s')^{-1}t^{-3/2}\exp\left[-\frac{(\mu_s')^{-2}}{4Dct}\right]\exp(-\mu_a ct)$$

Time resolved reflectometry: Approximation

- $\frac{d(\ln R)}{dt}$ represents the slope of the decay curve

$$-\frac{d}{dt}\ln(R(r,t)) = \mu_a c + \frac{5}{2t} - \frac{r^2 + (\mu_s')^{-2}}{4Dct^2} \approx \mu_a c \quad \text{as } t \to \infty$$

$$-\frac{d}{dt}\ln(R(t)) = \mu_a c + \frac{3}{2t} - \frac{(\mu_s')^{-2}}{4Dct^2} \approx \mu_a c \quad \text{as } t \to \infty$$

- At long times the behavior becomes dominated by $\boldsymbol{\mu_a}$

Time resolved reflectometry: Relation with μ_s'

The relation between
the reduced scattering coefficient μ_s' and
the time t_{max} at which the peak in time-resolved reflectance occurs at a collection site distant r from the source can be specified.

$$-\frac{d}{dt}ln\big(R(r,t)\big) = \mu_a c + \frac{5}{2t} - \frac{r^2 + (\mu_s')^{-2}}{4Dct^2} = 0$$

when $r >> \frac{1}{\mu_s'}$ the above equation can be stated as

$$\mu_s' = \mu_s(1-g) = \frac{1}{3r^2}(4\mu_a c^2 t_{max}^2 + 10ct_{max}) - \mu_a$$

Indirect methods:
3) Use of added absorbers

- Another method that can be used to evaluate both μ_a and μ_s' is the so called added absorber method.
- This method is destructive and can thus not be used *in vivo*.
  However, it is a very useful method for liquid tissue phantoms and for homogenized tissue.
- **The principle is to measure the fluence rate vs. the depth (to deduce μ_{eff}), add some absorber and redo the measurements etc.**

Indirect methods:
Use of added absorbers: Theory

The aim is to measure μ_{eff} for a number of added absorber concentrations (if the diffusion approximation is valid).

$$\mu_{eff}^{\ 2} = 3\mu_a(\mu_a + \mu_s')$$

with some added absorption $\mu_a = \mu_{a,t} + \mu_{a,d}$

for the tissue (t) and added dye (d), respectively.

If

$\mu_{a,t} + \mu_{a,d} \langle\langle \mu_s'$ then $\mu_{eff}^{\ 2} \approx 3(\mu_{a,t} + \mu_{a,d})\mu_s'$

Indirect methods:
Use of added absorbers: Plot

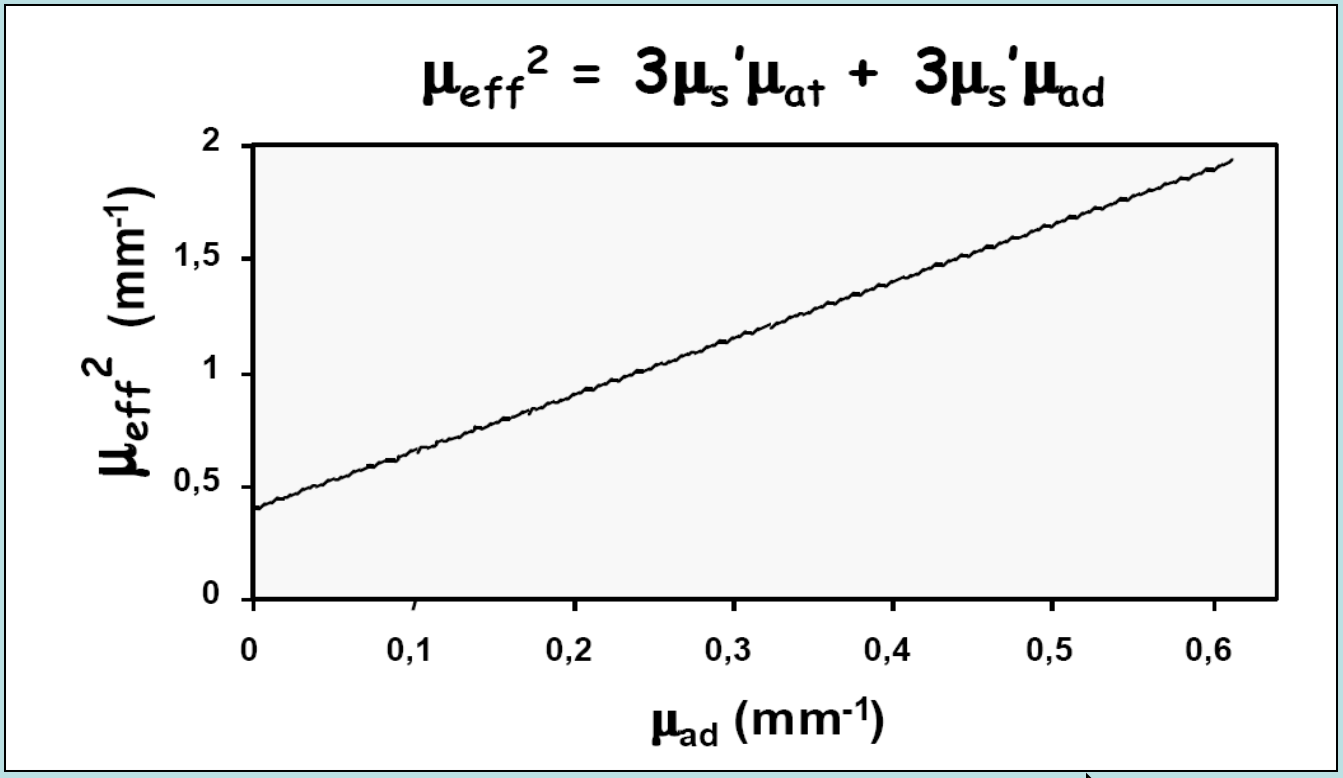

Slope = $3\mu_s'$; Y-intercept = $3\ \mu_s'\mu_{a,t}$ ⇒ $\mu_{a,t}$

Indirect methods: Absorber peak measurement

Evaluation of μ_a

- if the diffusion approximation is not valid
- but if the spectroscopy of the main absorber is known

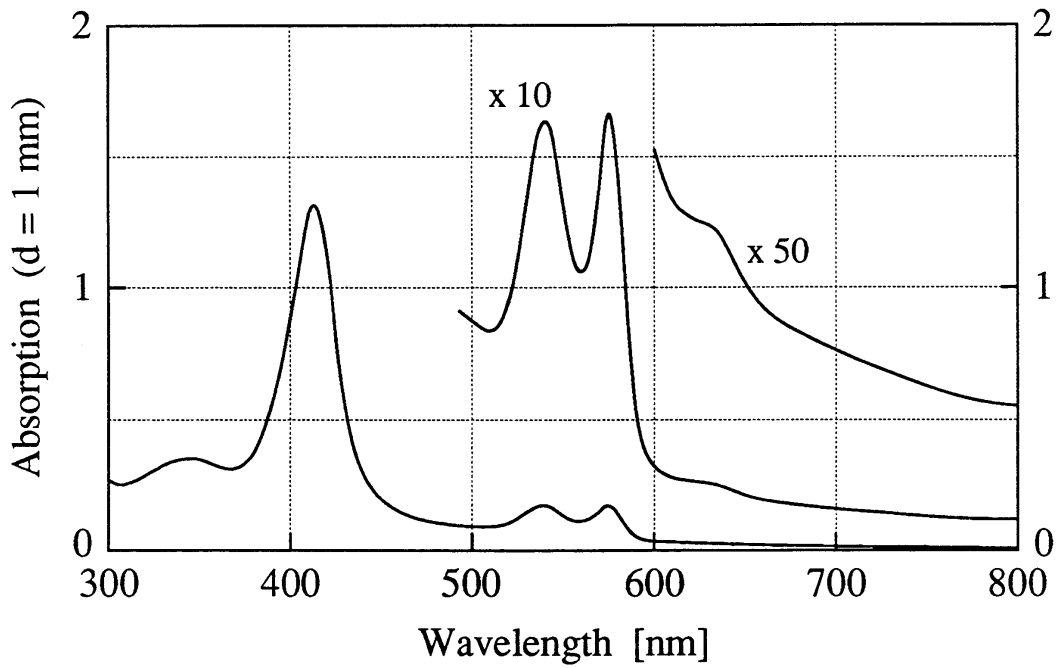

Absorption of diluted (1 %) human blood

Absorption Spectrometer

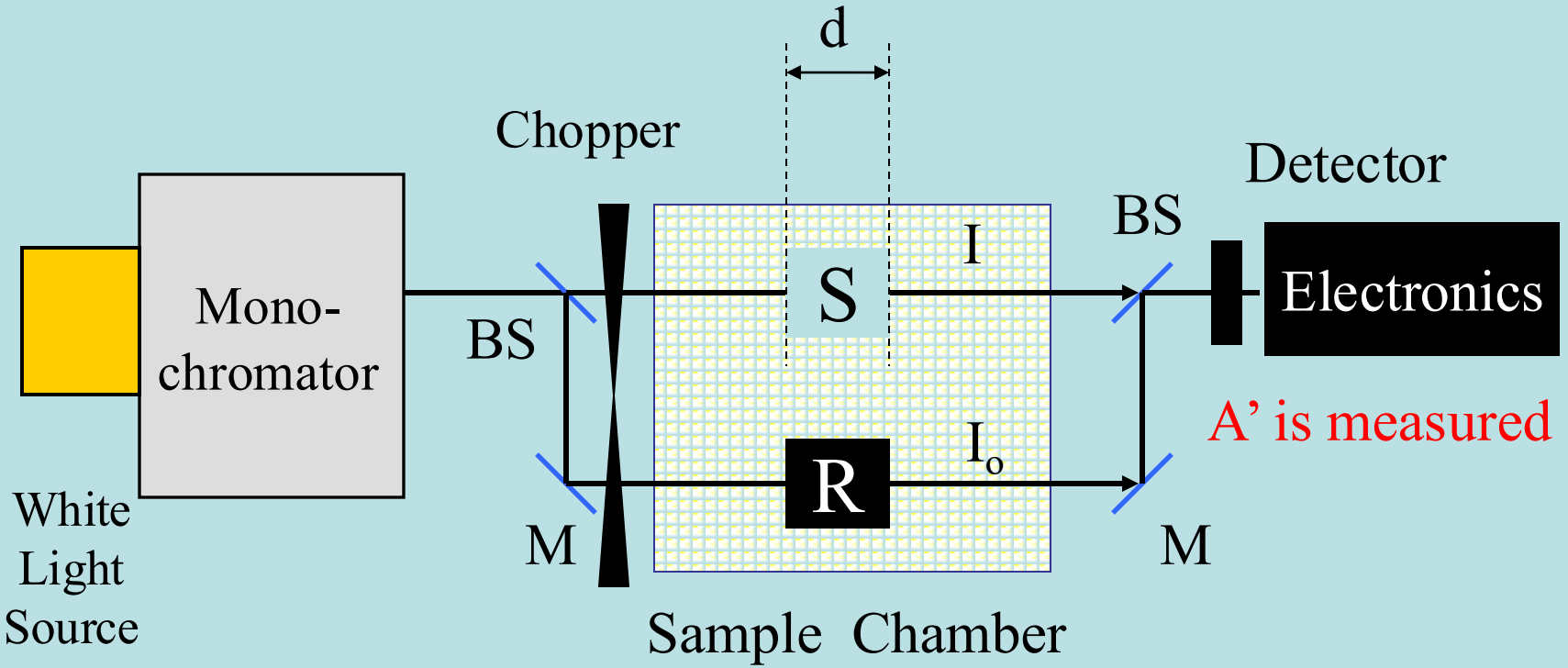

BS: beam splitter; M: mirror; S: sample; R: reference

In the absence of scattering: $\mu_a = 2.303 A'/d$

Indirect methods: Added absorbers
Evaluation of μ_a- example: beef muscle slice

Extinction of a beef muscle slice

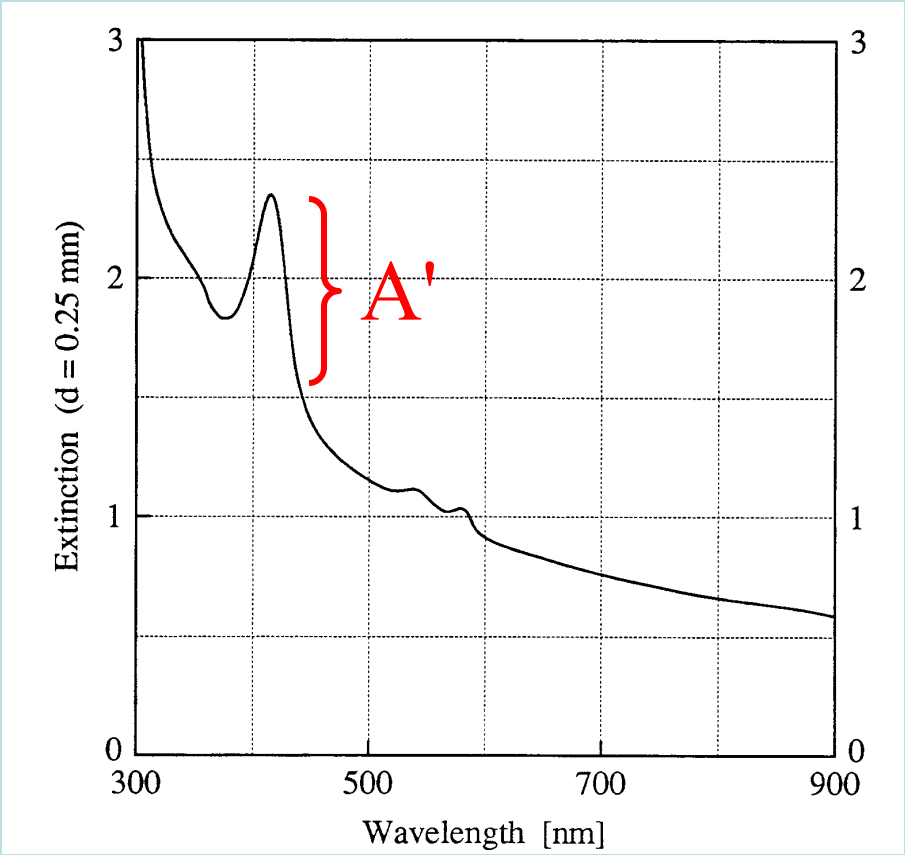

Main absorber: blood

μ_a (410 nm) > 2.303A'/d
= 7 mm^{-1}
= μ_{Hb} (410 nm)

External (R_d) and internal (μ_{eff}) measurements can be combined !

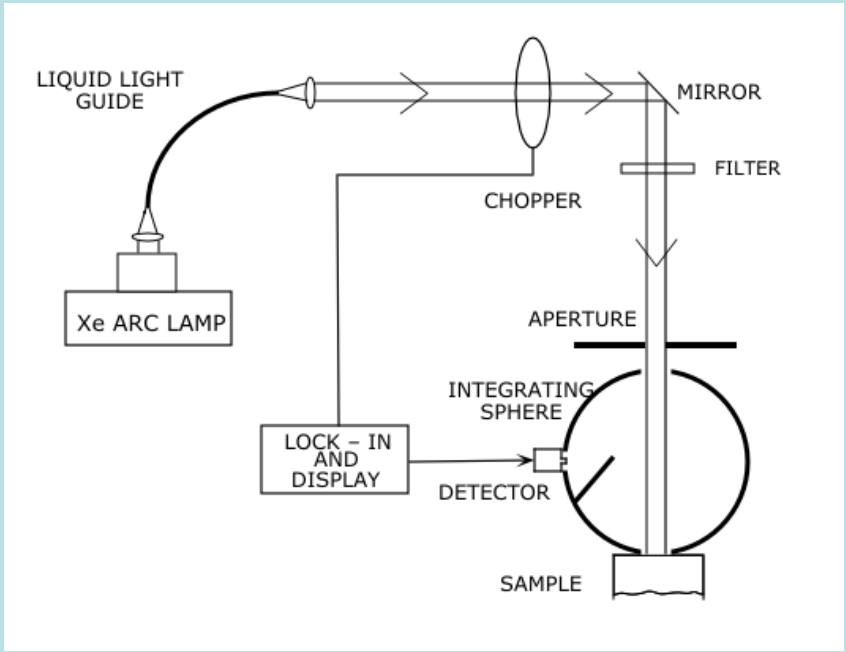

R_d

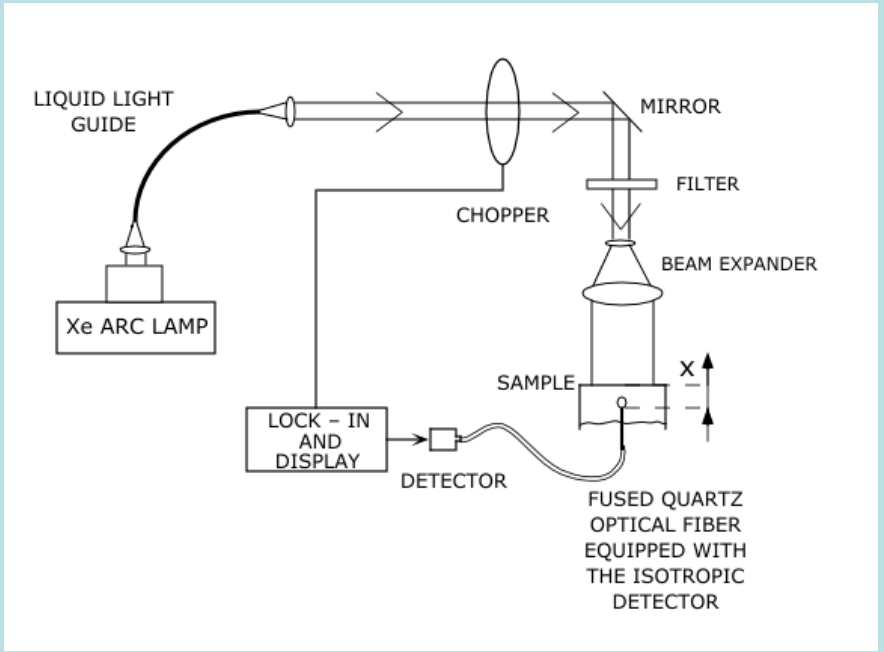

μ_{eff}

Diffuse reflectance and effective attenuation coefficient for different optical properties

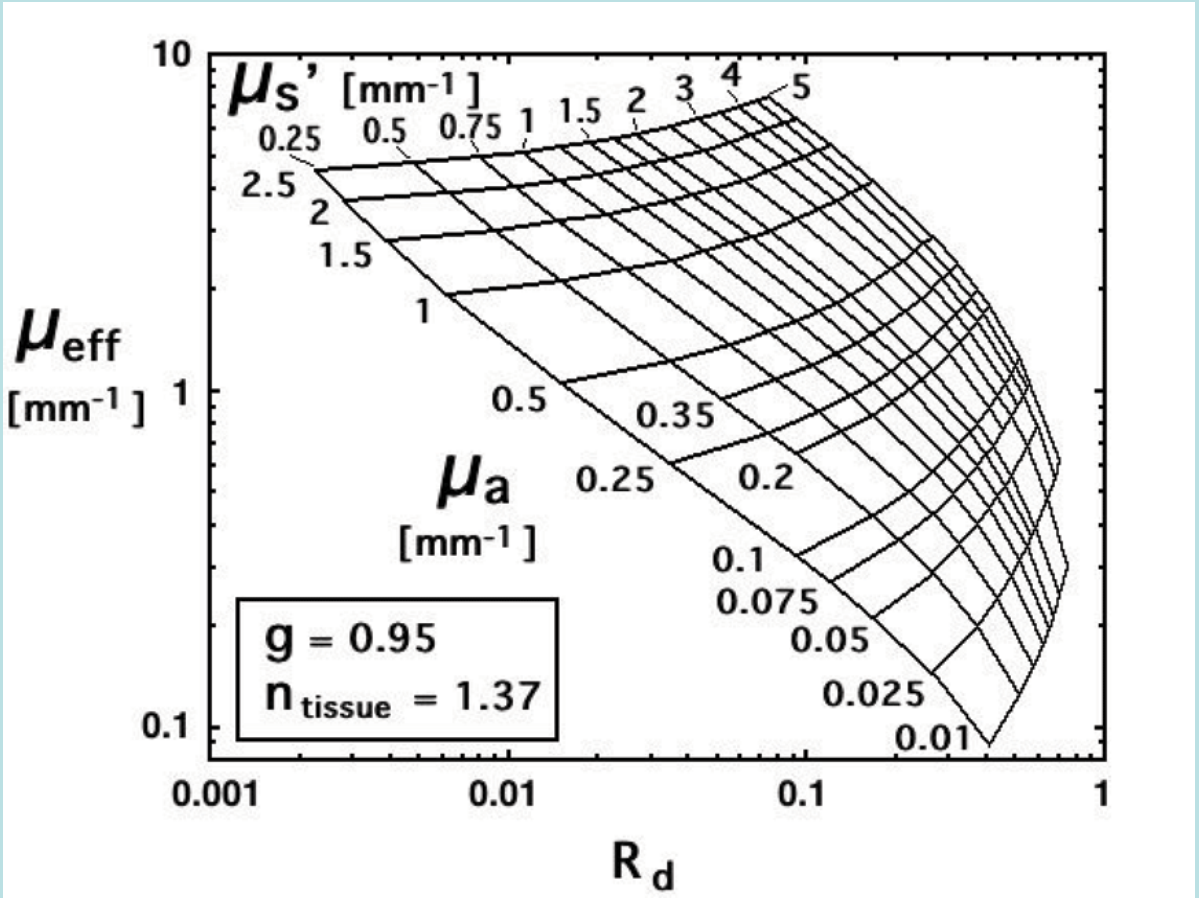

(grid generated by Monte-Carlo simulation)

Optical properties of the wall of an excised human esophagus

	λ [nm]		
	410	514	630
μ_a [mm^{-1}]	2.4	0.30	0.09
μ_s' [mm^{-1}]	5.0	1.4	0.7
K [mm^{-1}]	4.0	0.5	0.17
S [mm^{-1}]	3.0	1.0	0.5
μ_{eff} [mm^{-1}]	7.3	1.2	0.46
R_∞ [%]	9.4	17	24
k	2.6	3.5	4.2
$F(0)/E$	1.6	2.2	2.8

Source: G. Wagnières, EPFL Thesis Nr. 1024, 1992

Human tissue optical properties

Type	λ [nm]	μ_a [mm^{-1}]	μ_s [mm^{-1}]	μ_s' [mm^{-1}]	g
Aorta (media)	476	0.73	41	4.5	0.89
	514	0.7	47.4	4.3	0.91
	633	0.23	31	3.1	0.9
	1064	0.1	63.4	2.54	0.96
Bladder mucosa	456	1.3	13.3	1.73	0.87
	514	0.21	6.9	0.97	0.86
	630	0.1	11.3	1.7	0.85
	1064	0.07	7.5	1.25	0.85
Bladder wall	456	0.27	31.8	4.45	0.86
	514	0.3	22.1	3.1	0.86
	630	0.04	12.9	1.94	0.85
	1064	0.09	5.4	0.81	0.85
Brain (white matter)	456	0.81	92.3	7.38	0.92
	514	0.5	104.5	7.32	0.93
	630	0.15	38.6	5.4	0.86
	1064	0.16	51.3	2.05	0.96
Brain (gray matter)	456	0.9	68.6	3.43	0.95
	514	1.17	57.8	1.73	0.97
	630	0.14	47.3	3.31	0.93
	1064	0.19	26.7	1.34	0.95

Human tissue optical properties

Type	λ [nm]	μ_a [mm^{-1}]	μ_s [mm^{-1}]	μ_s' [mm^{-1}]	g
Fat (abdominal)	456	1	15.6	1.25	0.92
	514	0.42	9.9	1.19	0.88
	630	0.17	9.1	0.91	0.9
	1064	0.3	3.7	0.33	0.91
Kidney (pars conv.)	456	4.3	93	4.65	0.95
	514	1	38.1	1.14	0.97
	630	0.7	53.9	1.08	0.98
	1064	0.24	7.2	1.01	0.86
Kidney (medulla ren.)	456	2.7	128.3	3.85	0.97
	514	1.1	43.9	1.76	0.96
	630	0.7	63.1	1.26	0.98
	1064	0.21	7.7	0.23	0.97
Liver	456	3	109.7	5.49	0.95
	514	1.23	95.7	6.7	0.93
	630	0.53	52.3	2.62	0.95
	1064	0.07	35.6	1.78	0.95

Human tissue optical properties

Type	λ [nm]	μ_a [mm^{-1}]	μ_s [mm^{-1}]	μ_s' [mm^{-1}]	g
Muscle (M.soleus)	456	1.2	79.8	2.39	0.97
	514	1	38.5	1.93	0.95
	630	0.4	17.5	1.4	0.92
	1064	0.2	21.5	0.86	0.96
Oesophagus (tun. musc.)	456	0.78	34.1	3.75	0.89
	514	1.3	23.6	3.3	0.86
	630	0.53	13.6	1.9	0.86
	1064	0.11	8.3	1.16	0.86

References

A. Rogan, *Dosimetrie thermischer Laseranwendungen in der Medizin*, ecomed, 1997